

Stimulated Raman scattering of an *EH* waveguide mode near cyclotron resonance

Joseph E. Willett

Department of Physics and Astronomy, University of Missouri-Columbia, Columbia, Missouri 65211

Yildirim Aktas

Department of Physics, University of North Carolina at Charlotte, Charlotte, North Carolina 28223

Behrouz Maraghechi

*The Center for Theoretical Physics and Mathematics, Atomic Energy Organization of Iran, Tehran, Iran
and Department of Physics, Amir Kabir University, Tehran, Iran*

Hassan Mehdian

Department of Physics, Teacher Training University, Tehran, Iran

(Received 4 October 1993)

The stimulated backscattering of a predominantly transverse magnetic waveguide mode off of a space-charge wave in a plasma-filled waveguide is investigated. A formula is derived for the growth rate of the backscattered wave and scatterer wave with the pump wave frequency near the electron cyclotron frequency. A numerical study indicates that the phase-matching conditions permit the approach to cyclotron resonance with substantial enhancement of the growth rate. Possible use of the *EH* waveguide mode as a pump for a free electron laser is discussed.

PACS number(s): 41.60.Cr, 52.35.Mw, 52.40.Fd, 52.75.Ms

An intense electromagnetic wave propagating in a plasma may undergo stimulated Raman backscattering. This parametric instability phenomenon may occur, e.g., in a waveguide containing a plasma or an electron beam. In this paper we study backscattering of a lower-branch *EH* waveguide mode off of a space-charge wave in a plasma-filled, cylindrical, metallic waveguide containing a uniform, static, axial magnetic field. The *EH* modes are the TM modes of an empty waveguide modified by the presence of the gyromagnetic medium [1]. A cylindrical coordinate system (r, θ, z) is introduced with the z axis taken as the axis of the guide. The pump wave (ω_1, k_1) is propagating in the negative z direction with a frequency ω_1 which is near (but not exactly equal to) the electron cyclotron frequency ω_c . The space-charge scatterer wave (ω_2, k_2) is propagating in the negative z direction with a phase velocity sufficiently small compared to the speed of light c to permit invoking the electrostatic approximation. The backscattered wave $(\omega_3, 0)$ is a lower-branch *EH* waveguide mode which is sufficiently near cutoff to be purely transverse magnetic with a wave number k_3 which is virtually zero.

The axial component \tilde{E}_z of the total electric field for the three axially symmetric waves may be written in the form

$$\tilde{E}_z = \sum_{j=1}^3 (\tilde{E}_{zj} + \text{c.c.}), \quad (1)$$

where

$$\tilde{E}_{z1} = E_{z10} [f_a Z_0(\kappa_a r) + f_b Z_0(\kappa_b r)] \exp[i(k_1 z + \omega_1 t)], \quad (2)$$

$$\tilde{E}_{z2} = E_{z20} J_0(p_{0\nu} r / R) \exp[i(k_2 z + \omega_2 t)], \quad (3)$$

$$\tilde{E}_{z3} = E_{z30} J_0(p_{0\nu} r / R) \exp[-i\omega_3 t], \quad (4)$$

$$f_a + f_b = 1, \quad (5)$$

$$Z_n(\kappa_\mu r) = \begin{cases} J_n(|\kappa_\mu| r), & \kappa_\mu^2 > 0 \\ I_n(|\kappa_\mu| r), & \kappa_\mu^2 < 0 \end{cases} \quad (\mu = a, b). \quad (6)$$

The radial dependence of the axial component of the *EH* pump wave is expressed as a linear combination of two Bessel functions. In the presence of a uniform, static, axial magnetic field of finite magnitude, transverse electron motions exist and this mode possesses a longitudinal magnetic as well as a longitudinal electric wave field. Consequently, two Bessel functions are required to satisfy the boundary conditions (see Ref. [1] and references contained therein). The radial dependence for the scatterer and the scattered waves is expressed by a single Bessel function. All of these Bessel functions are of the first kind and of order zero, I_0 is a modified Bessel function, $p_{0\nu}$ is the ν th zero of J_0 , and R is the waveguide inner radius. Wave numbers k_1 and k_2 , frequency ω_1 , and the real parts of frequencies ω_2 and ω_3 are positive. The appropriate phase-matching conditions are

$$\omega_1 = \omega_2 + \omega_3, \quad (7)$$

$$k_1 = k_2. \quad (8)$$

This stimulated Raman scattering process may be interpreted as the decay of a pump photon (ω_1, k_1) into a plasmon (ω_2, k_2) and a scattered photon $(\omega_3, 0)$. Equations (7) and (8) express the conservation of energy and momentum, respectively.

A nonlinear wave equation may be derived from the electron continuity, electron momentum transfer, and Maxwell equations in the form

$$\left\{ \frac{\partial^2}{\partial t^2} \left[\frac{\partial^2}{\partial t^2} + \omega_p^2 \right] \left[\frac{1}{c^2} \frac{\partial^2}{\partial t^2} - \nabla^2 + \frac{\omega_p^2}{c^2} \right]^2 + \omega_c^2 \left[\frac{1}{c^2} \frac{\partial^2}{\partial t^2} - \nabla^2 \right] \left[\left[\frac{\partial^2}{\partial t^2} + \omega_p^2 \right] \left[\frac{1}{c^2} \frac{\partial^2}{\partial t^2} - \frac{\partial^2}{\partial z^2} \right] - \frac{\partial^2}{\partial t^2} \nabla_1^2 \right] \right\} \tilde{E}_z = \mathcal{N}, \quad (9)$$

where ω_p is the plasma frequency. The derivation and nonlinear terms \mathcal{N} are presented in Ref. [2]. The linear dispersion relation for the real part of the frequency ω_{2r} and wave number k_2 of the space-charge wave may be obtained from this wave equation. Introducing Eq. (3), neglecting nonlinear terms \mathcal{N} , and invoking the electrostatic approximation (i.e., neglecting terms containing $1/c^2$) yields

$$\frac{k_2^2 R^2}{p_{0v}^2} = \frac{\omega_{2r}^2 (\omega_c^2 + \omega_p^2 - \omega_{2r}^2)}{(\omega_c^2 - \omega_{2r}^2)(\omega_p^2 - \omega_{2r}^2)}. \quad (10)$$

The real part of the frequency ω_{3r} of the lower branch of the *EH* waveguide mode at cutoff, obtained by introducing Eq. (4) into the linearized equation (9), is given by

$$\omega_{3r}^2 = \omega_p^2 + p_{0v}^2 R^{-2} c^2. \quad (11)$$

In order to derive the temporal growth rate γ for exponentially growing waves 2 and 3, the linearized solution for each of the three interacting waves is introduced into the nonlinear terms of Eq. (9). For simplicity, only the terms in \mathcal{N} which become large near cyclotron resonance will be retained. The transverse electron velocity components for the pump wave may be expressed in the form

$$\tilde{u}_{r1} = \frac{|e| \omega_1 E_{z10} Z_1(\kappa_\mu r) \exp[i(k_1 z + \omega_1 t)]}{m_0 k_1 (\omega_c^2 - \omega_1^2)} \sum_\mu \frac{f_\mu}{|\kappa_\mu|} \left\{ \kappa_\mu^2 - \frac{(\omega_1^2 - \omega_p^2)}{c^2} \left[\frac{2(k_1^2 + \kappa_\mu^2 - \omega_1^2 c^{-2}) + \omega_p^2 c^{-2}}{k_1^2 + \kappa_\mu^2 - \omega_1^2 c^{-2}} \right] \right\}, \quad (12)$$

$$\tilde{u}_{\theta 1} = - \frac{i|e| \omega_c E_{z10} Z_1(\kappa_\mu r) \exp[i(\kappa_1 z + \omega_1 t)]}{m_0 k_1 (\omega_c^2 - \omega_1^2)} \sum_\mu \frac{f_\mu}{|\kappa_\mu|} \left\{ \kappa_\mu^2 - \frac{(\omega_1^2 - \omega_p^2)}{c^2} \left[\frac{(1 + \omega_1^2 \omega_c^{-2})(k_1^2 + \kappa_\mu^2 - \omega_1^2 c^{-2}) + \omega_1^2 \omega_c^{-2} \omega_p^2 c^{-2}}{k_1^2 + \kappa_\mu^2 - \omega_1^2 c^{-2}} \right] \right\}, \quad (13)$$

where $|e|$ is the magnitude of the electron charge and m_0 is the electron (rest) mass. Note that these transverse velocity components become larger when ω_1 approaches ω_c . With Eqs. (1)–(4) inserted into the left-hand side of Eq. (9) and the phase-matching conditions employed in the \mathcal{N} terms, the sums of terms of like phase on the two sides may be equated. That is, the sum of terms containing $\exp[i(k_2 z + \omega_2 t)]$ on the left may be equated to the sum of terms containing $\exp[i(k_1 z + \omega_1 t)]$ times $\exp[-i\omega_3 t]$ on the right; the sum containing $\exp[-i\omega_3 t]$ on the left may be equated to the sum containing $\exp[-i(k_1 z + \omega_1 t)]$ times $\exp[i(k_2 z + \omega_2 t)]$ on the right. The radial dependence of the pump wave may be treated by the method of Ref. [3].

The foregoing procedure yields the following two linear, homogeneous equations for the wave amplitudes E_{z20} and E_{z30} :

$$(p_{0v}^2 R^{-2} + k_2^2) \{ \omega_2^2 (\omega_2^2 - \omega_p^2) (p_{0v}^2 R^{-2} + k_2^2) + \omega_c^2 [k_2^2 (\omega_p^2 - \omega_2^2) - \omega_2^2 p_{0v}^2 R^{-2}] \} E_{z20} = \frac{i|e| k_1 \omega_2 \omega_p^2 E_{z10} E_{z30} S_2}{m_0 \omega_{3r} (\omega_c^2 - \omega_1^2)} \quad (14)$$

$$-\omega_3^2 (p_{0v}^2 R^{-2} + \omega_p^2 c^{-2} - \omega_3^2 c^{-2}) [(\omega_p^2 - \omega_3^2) (p_{0v}^2 R^{-2} + \omega_p^2 c^{-2} - \omega_3^2 c^{-2}) + \omega_c^2 (p_{0v}^2 R^{-2} - \omega_3^2 c^{-2})] E_{z30} = \frac{i|e| \omega_1 \omega_p^2 \omega_{3r} E_{z10}^* E_{z20} S_3}{m_0 \omega_{2r} k_1 (\omega_c^2 - \omega_1^2) c^2}. \quad (15)$$

Here, E_{z10}^* is the complex conjugate of E_{z10} , and S_2 and S_3 are given by

$$S_2 = \sum_\mu f_\mu \left\{ \omega_1 \omega_{2r} \left[\kappa_\mu^2 - \frac{(\omega_1^2 - \omega_p^2)}{c^2} \frac{2(k_1^2 + \kappa_\mu^2 - \omega_1^2 c^{-2}) + \omega_p^2 c^{-2}}{k_1^2 + \kappa_\mu^2 - \omega_1^2 c^{-2}} \right] \times [(k_1^2 + 3p_{0v}^2 R^{-2} + \kappa_\mu^2) \alpha_{1\mu} - 2p_{0v}^2 R^{-3} |\kappa_\mu|^{-1} \alpha_{2\mu} - 2p_{0v} R^{-2} \alpha_{3\mu} - p_{0v} R^{-1} |\kappa_\mu|^{-1} (k_1^2 + p_{0v}^2 R^{-2} + 3\kappa_\mu^2) \alpha_{4\mu} + 4p_{0v} R^{-3} |\kappa_\mu|^{-1} \alpha_{5\mu}] + \omega_c^2 \left[\kappa_\mu^2 - \frac{(\omega_1^2 - \omega_p^2)}{c^2} \frac{(1 + \omega_1^2 \omega_c^{-2})(k_1^2 + \kappa_\mu^2 - \omega_1^2 c^{-2}) + \omega_1^2 \omega_c^{-2} \omega_p^2 c^{-2}}{k_1^2 + \kappa_\mu^2 - \omega_1^2 c^{-2}} \right] \times [(k_1^2 + 3p_{0v}^2 R^{-2} + \kappa_\mu^2) \alpha_{1\mu} - 2p_{0v}^2 R^{-3} |\kappa_\mu|^{-1} \alpha_{2\mu} - 2p_{0v} R^{-2} \alpha_{3\mu} - p_{0v} R^{-1} |\kappa_\mu|^{-1} (k_1^2 + p_{0v}^2 R^{-2} + 3\kappa_\mu^2) \alpha_{4\mu} + 4p_{0v} R^{-3} |\kappa_\mu|^{-1} \alpha_{5\mu}] \right\}, \quad (16)$$

$$S_3 = \sum_{\mu} \frac{f_{\mu} p_{0\nu}}{|\kappa_{\mu}| R} \left\{ \kappa_{\mu}^2 - \frac{(\omega_1^2 - \omega_p^2)}{c^2} \left[\frac{2(k_1^2 + \kappa_{\mu}^2 - \omega_1^2 c^{-2}) + \omega_p^2 c^{-2}}{k_1^2 + \kappa_{\mu}^2 - \omega_1^2 c^{-2}} \right] \right\} \\ \times \{ c^{-2} [\omega_c^2 \omega_{3r}^2 - (\omega_{3r}^2 - \omega_p^2)^2] \alpha_{4\mu} + (\omega_c^2 - \omega_{3r}^2 + \omega_p^2) [2p_{0\nu} |\kappa_{\mu}| R^{-1} \alpha_{1\mu} - 2p_{0\nu} R^{-2} \alpha_{2\mu} \\ - 2|\kappa_{\mu}| R^{-1} \alpha_{3\mu} - (p_{0\nu}^2 R^{-2} + \kappa_{\mu}^2) \alpha_{4\mu} + 4R^{-2} \alpha_{5\mu}] \}, \quad (17)$$

$$\alpha_{1\mu} = 2R^{-2} [J_1(p_{0\nu})]^{-2} \int_0^R r [J_0(p_{0\nu} r / R)]^2 Z_0(\kappa_{\mu} r) dr, \quad (18)$$

$$\alpha_{2\mu} = 2R^{-1} [J_1(p_{0\nu})]^{-2} \int_0^R [J_0(p_{0\nu} r / R)]^2 Z_1(\kappa_{\mu} r) dr, \quad (19)$$

$$\alpha_{3\mu} = 2R^{-1} [J_1(p_{0\nu})]^{-2} \int_0^R J_0(p_{0\nu} r / R) J_1(p_{0\nu} r / R) Z_0(\kappa_{\mu} r) dr, \quad (20)$$

$$\alpha_{4\mu} = 2R^{-2} [J_1(p_{0\nu})]^{-2} \int_0^R r J_0(p_{0\nu} r / R) J_1(p_{0\nu} r / R) Z_1(\kappa_{\mu} r) dr, \quad (21)$$

$$\alpha_{5\mu} = 2 [J_1(p_{0\nu})]^{-2} \int_0^R r^{-1} J_0(p_{0\nu} r / R) J_1(p_{0\nu} r / R) Z_1(\kappa_{\mu} r) dr. \quad (22)$$

The summation over μ contains two terms, $\mu=a$ and $\mu=b$. Simplification of the left-hand side of Eqs. (14) and (15) may be achieved by expressing the complex frequencies ω_2 and ω_3 in the form

$$\omega_2 = \omega_{2r} - i\gamma, \quad (23)$$

$$\omega_3 = \omega_{3r} + i\gamma, \quad (24)$$

introducing Eqs. (10) and (11), and retaining only terms of first order in γ . The necessary and sufficient condition for a nontrivial solution of these two linear, homogeneous equations then yields the growth rate

$$\gamma = \frac{|e| |E_{z10}| \omega_p c}{2m_0 \omega_{3r} \omega_c (p_{0\nu}^2 R^{-2} + k_1^2) |\omega_c^2 - \omega_1^2|} \\ \times \left[\frac{\omega_1 S_2 S_3}{\omega_{2r} (\omega_c^2 + \omega_p^2 - 2\omega_{2r}^2)} \right]^{1/2}. \quad (25)$$

In order to illustrate that phase matching is possible near cyclotron resonance, calculations were made with

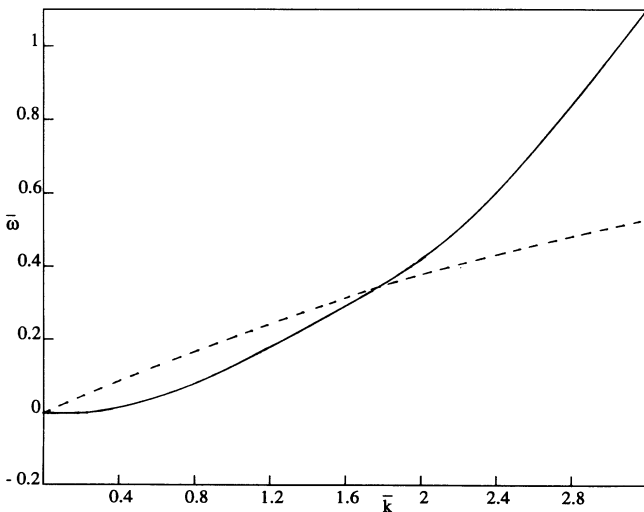


FIG. 1. Dimensionless frequency $\bar{\omega}_2$ vs dimensionless wave number \bar{k}_2 (dashed curve) and dimensionless beat frequency $\bar{\omega}_1 - \bar{\omega}_3$ vs dimensionless wave number \bar{k}_1 (solid curve). The dimensionless cyclotron frequency $\bar{\omega}_c = 10$.

dimensionless waveguide inner radius $\bar{R} = R\omega_p/c = 0.6671$ and $p_{0\nu} = p_{01} = 2.405$. The dispersion curves for the first mode ($\nu=1$) of the EH pump wave and space-charge wave were computed by a method equivalent to that of Ivanov and Alexov [1]. Figures 1, 2, and 3 show the dimensionless (real) frequency $\bar{\omega}_2 = \omega_{2r}/\omega_p$ as a function of the dimensionless wave number $\bar{k}_2 = k_2 c/\omega_p$ for the space-charge wave. These figures also show the dimensionless (real) beat frequency

$$\bar{\omega}_1 - \bar{\omega}_3 = \omega_1/\omega_p - \omega_{3r}/\omega_p$$

for the EH_{01} pump wave and scattered wave as a function of the dimensionless wave number $\bar{k}_1 = k_1 c/\omega_p$. In Fig. 1, the dimensionless cyclotron frequency is $\bar{\omega}_c = \omega_c/\omega_p = 10$. The point of intersection gives the phase-matched values with $\omega_1/\omega_c = 0.233$. In Fig. 2, $\bar{\omega}_c$ has been lowered to 4.47. This pushes the EH_{01} mode frequency $\bar{\omega}_1$ down, thereby moving the intersection point of the $\bar{\omega}_2$ and $\bar{\omega}_1 - \bar{\omega}_3$ curves toward higher values of \bar{k}_1 and \bar{k}_2 where $\omega_1/\omega_c = 0.947$. In Fig. 3, $\bar{\omega}_c = 4.46$ and the $\bar{\omega}_1 - \bar{\omega}_3$ curve has been pushed down so far that it will not intersect the $\bar{\omega}_2$ curve. For the value of \bar{R} chosen here, phase matching can occur with the pump frequency within approximately 5% of the cyclotron frequency when $\bar{\omega}_c = 4.47$ but not when $\bar{\omega}_c \leq 4.46$. In Fig. 4, the dimensionless growth rate

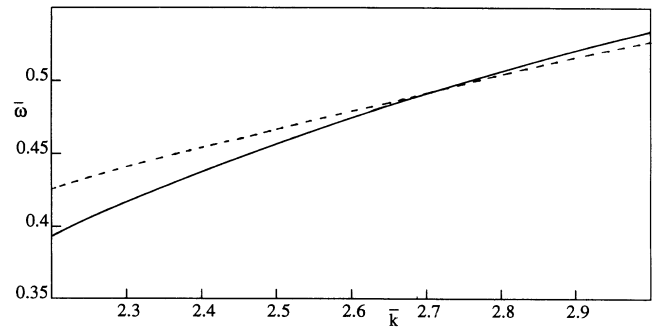


FIG. 2. Dimensionless frequency $\bar{\omega}_2$ vs dimensionless wave number \bar{k}_2 (dashed curve) and dimensionless beat frequency $\bar{\omega}_1 - \bar{\omega}_3$ vs dimensionless wave number \bar{k}_1 (solid curve). The dimensionless cyclotron frequency $\bar{\omega}_c = 4.47$.

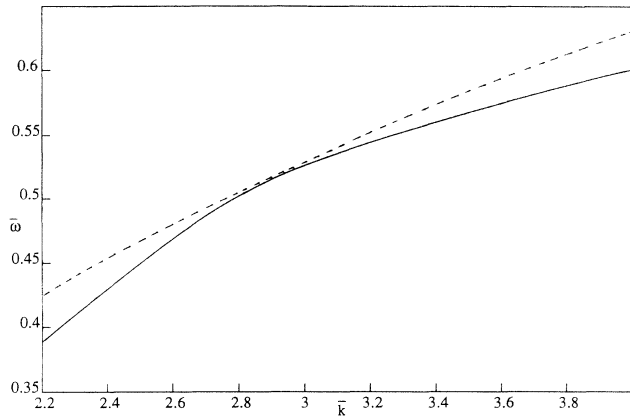


FIG. 3. Dimensionless frequency $\bar{\omega}_2$ vs dimensionless wave number \bar{k}_2 (dashed curve) and dimensionless frequency $\bar{\omega}_1 - \bar{\omega}_3$ vs dimensionless wave number \bar{k}_1 (solid curve). The dimensionless cyclotron frequency $\bar{\omega}_c = 4.46$.

$$\bar{\gamma} = \gamma m_0 c / (2|e||E_{z10}|)$$

is shown as a function of $\bar{\omega}_c$. For $\bar{\omega}_c = 17.6, 8, 5, 4.6,$ and 4.47 ; $\bar{\omega}_1 = 4.098, 4.099, 4.12, 4.16,$ and 4.23 ; and $\bar{\omega}_2 = 0.356, 0.357, 0.380, 0.416,$ and 0.491 , respectively. Note that significant enhancement of the growth rate occurs when the pump is near cyclotron resonance, i.e., when the pump wave frequency ω_1 is approximately equal to the cyclotron frequency ω_c . The electrons then become synchronized with the pump wave and the transverse velocity components which contain the factor $(\omega_c^2 - \omega_1^2)^{-1}$ become very large. Since this factor also appears in the growth rate equation, γ is enhanced near cyclotron resonance.

The plasma waveguide is an essential component in many plasma electronic devices. Its use requires knowledge of the properties of the eigenmodes. The present paper illustrates one characteristic of the EH_{01} mode, namely, its propensity to undergo parametric decay. This may impose a limitation on the intensity of the mode which may be employed and also a limitation on the system parameter range. The use of EH modes (i.e.,

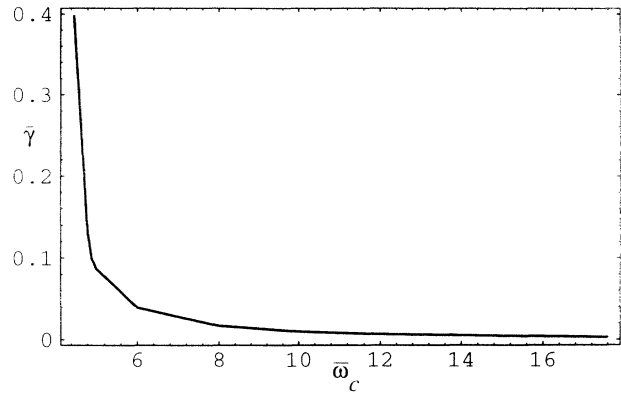


FIG. 4. Dimensionless growth rate $\bar{\gamma}$ vs dimensionless cyclotron frequency $\bar{\omega}_c$.

TM modes modified by a finite axial magnetic field) in free electron lasers has been suggested. They may be generated in a relativistic electron beam by either a longitudinal electrostatic wiggler [4,5] or a conventional magnetic wiggler [6]. The present study shows that an intensity or parameter range limitation may also arise in this application.

A free electron laser may employ an electromagnetic pump wave as an alternative to the conventional wiggler consisting of a static, spatially periodic, transverse magnetic field. The analysis of Sprangle and Granatstein [7] has shown that the growth rate for the stimulated backscattering of an electromagnetic wave by a relativistic electron beam is enhanced when the wave is near cyclotron resonance. The present analysis indicates that the lower-branch EH_{01} waveguide mode can backscatter when it is near cyclotron resonance with considerable enhancement of the growth rate. This suggests that this waveguide mode would be suitable as a pump wave for a free electron laser. Fliflet and Manheimer [8] have recently designed an experiment which would employ a TE waveguide mode as a wiggler. The present study suggests that the use of an EH mode might provide an alternative type of wiggler with unique (cyclotron resonance) advantages.

- [1] S. T. Ivanov and E. G. Alexov, *J. Plasma Phys.* **43**, 51 (1990).
- [2] P. Uddholm, J. E. Willett, and S. Bilikmen, *J. Phys. D* **24**, 1278 (1991).
- [3] P. Uddholm, *J. Phys. D* **24**, 1270 (1991).
- [4] G. Bekefi, *J. Appl. Phys.* **51**, 3081 (1980).
- [5] D. L. Fenstermacher and C. E. Seyler, *Phys. Fluids* **30**,

190 (1987).

- [6] H. P. Freund and A. K. Ganguly, *Phys. Rev. A* **28**, 3438 (1983).
- [7] P. Sprangle and V. L. Granatstein, *Appl. Phys. Lett.* **25**, 377 (1974).
- [8] A. W. Fliflet and W. M. Manheimer, *Bull. Am. Phys. Soc.* **38**, 1964 (1993).